EXPERIMENTAL INVESTIGATION ON THE HEAT TRANSFER PERFORMANCE OF GALINSTAN LIQUID METAL DRIVEN BY ELECTROMAGNETISM

Fajing Li[1,2], Zhongkai Zhang[2]*, Sanmu Xie[1], Peizhu Chen[1]

[1]Joint Laboratory of Energy Saving and Intelligent Maintainence for Modern Transportations, No 100, Qinglong Road, Guangzhou 510430, Guangdong, P.R. China.

[*2]State Key Laboratory for Manufacturing Systems Engineering, Institute of Precision Engineering, School of Mechanical Engineering, Xi'an Jiaotong University, Xi'an 710049, P.R. China.

[*] Corresponding author: Zhongkai Zhang;

E-mail: zhangzk@xjtu.edu.cn

Liquid metals have excellent heat transfer performance and unique electromagnetic characteristics, providing new visions for cooling the high-speed motorized spindle shaft. Liquid metal can be driven by the magnetic field of the motor stator to induce current with no dynamic seal problem. In the present study, a shaft cooling structure of a motorized spindle with Galinstan liquid metal as the working fluid was designed and the heat transfer performance of the designed structure was investigated experimentally. The obtained results at the rated speed and rated current show that the induced voltage in the wire installed on the shaft reaches 1.2V, which can circulate the liquid metal in an 8 mm diameter copper pipe. In this case, its equivalent thermal conductivity reaches $8.1*10^4$ $W{\cdot}m^{-1}{\cdot}℃^{1}$*, which can effectively reduce the temperature of the motorized spindle rotor and make the temperature distribution of the motorized spindle more uniform.*

Keywords: *Galinstan liquid metal, shaft cooling, electromagnetic drive, heat transfer performance.*

1 Introduction

Studies show that thermal deformation in high-speed and high-precision machining may lead to machine tool errors of up to 40%-70% [1]. The high-speed motorized spindle is the main heat source and core component of CNC machine tools and is significantly prone to thermal problems. Generally, heat sources of a motorized spindle include bearings, motor stator, and motor rotor. In order to effectively reduce the temperature rise of the motorized spindle, numerous methods such as aerostatic (hydrostatic) bearings [2-3], oil-air lubrication technology [4-5], and spiral cooling water jacket technology for motor stator [6] have been proposed. However, these schemes and technologies only have a good cooling effect on the motor stator and bearing, resulting in prominent thermal problems in the shaft and motor rotor.

An innovative solution to cool the rotor system of a motorized spindle efficiently while reducing the thermal deformations is to connect the coolant to the shaft. In this regard, the

motorized spindle with a multi-cooling channel circuit [7] and the U-cooling channel in the shaft [8] have been proposed. Although remarkable achievements have been obtained in this way, the difficulty of high-pressure rotary dynamic seal increases sharply with the rotating speed, thereby limiting the application of this technology in engineering applications. Accordingly, this method is mostly used in the low- and medium-speed motorized spindles. To avoid the challenges of high-pressure dynamic seal and shaft cooling of a high-speed motorized spindle, Li [9] employed the two-phase loop thermosyphon to transfer the generated heat in the shaft. Further investigations revealed that this self-powered method can reduce the temperature rise by 44%. Zhang[10] numerically studied the thermal characteristics of spiral cooling motorized spindle and compared it with a U-shaped cooling motorized spindle. Results showed that compared to the U-shaped cooling system with a 7 mm cooling channel, the spiral cooling system under the same conditions has a lower temperature and a greater radial thermal deformation.

However, there is a temperature difference of tens of degrees of Celsius between the evaporation and condensation sections when the heat pipe operates normally, resulting in a poor cooling effect. Moreover, the vapor-liquid phase change of the circulating flow in the heat pipe affects the dynamic balance of the shaft. Consequently, the shaft is still the thermal weak link of a high-speed motorized spindle.

As new high-efficiency heat management working medium, Galinstan liquid metal has excellent heat transfer performance and unique electromagnetic driving characteristics, which provides new visions for motorized spindle cooling.

In a magnetic field, an electrified wire will be subjected to Ampere's force. Therefore, when liquid metal is subjected to an appropriate magnetic field and current conditions, it promotes and transfers the heat of the shaft. Fig. 1 shows that a central hole and several outer axial holes are machined in the studied rotating shaft. Moreover, radial holes are machined to connect the central hole to outer holes, forming circulation channels for liquid Galinstan. A pair of symmetrically placed wires are fixed on the shaft near the motor rotor. Electromagnets are arranged at the end of each wire and connect with it. The wire is led out by an electromagnet and rotates 90 degrees along the circumferential direction of the shaft and then connects to the central hole.

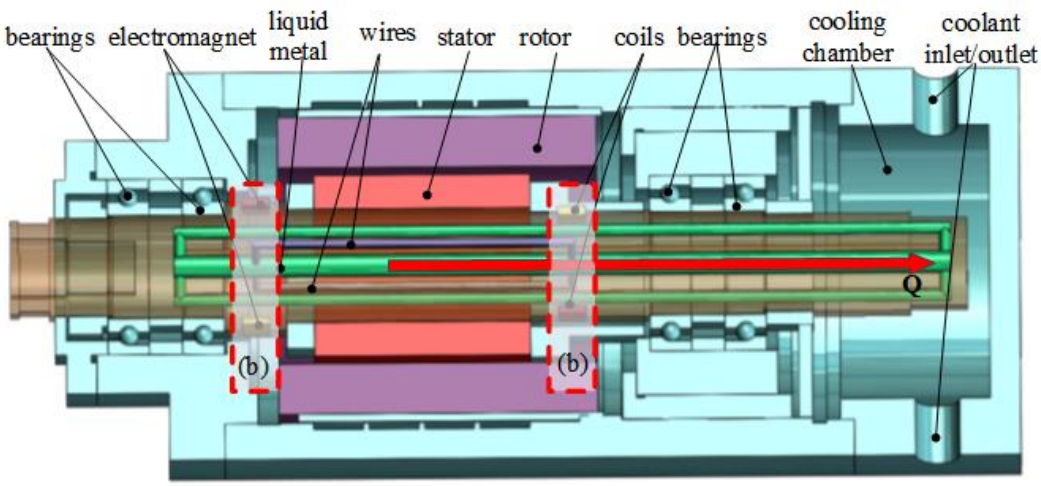

(a) Structure of liquid metal-cooled shaft of the motorized spindle

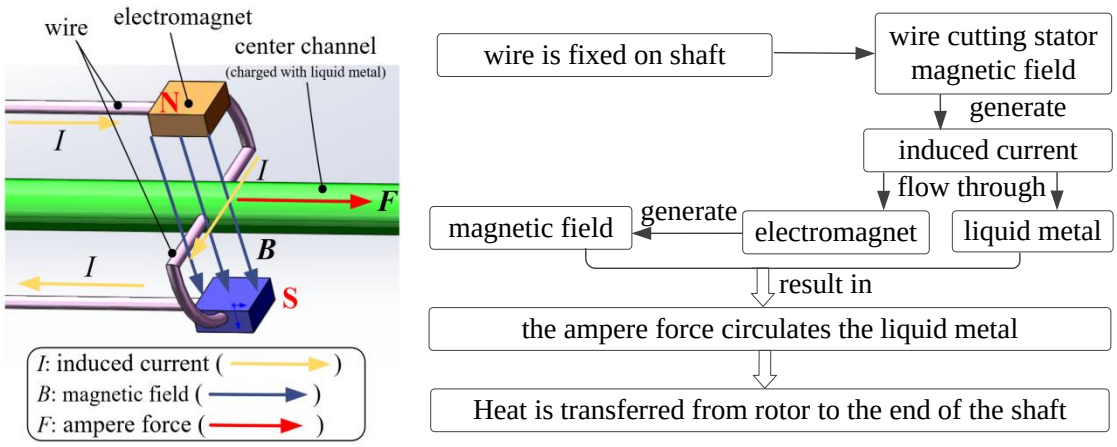

(b) Layout of the electromagnet and conductor

(c) Cooling process of the shaft with electromagnetically driven liquid metal structure

Fig. 1 The structure and cooling process of the motorized spindle with an electromagnetically driven liquid metal structure in the shaft

Fig. 1(b) schematically shows Ampere's force of an electrified wire in a magnetic field. When the motorized spindle is running, there is a speed difference between the rotating shaft and the magnetic field of the motor stator, which fixes the wire on the shaft cut of the stator magnetic field and induces a current in the wire. The induced current then flows through the electromagnet and induces a secondary magnetic field. Since the wire is led out by the electromagnet and rotates 90 degrees along the circumferential direction of the shaft, the current direction that flows through the liquid metal is perpendicular to the main magnetic field. Therefore, the liquid metal will be driven by the Ampere's force, and a circular flow forms. Subsequently, the liquid metal quickly absorbs the heat generated by the motor and bearing and transfers heat to the shaft end, and cools in the cooling chamber.

Reviewing the literature indicates that numerous investigations have been carried out on the flow and heat transfer characteristics of liquid metal. In this regard, The comparative study of Xiang's research[11] confirmed that compared to water, the thermal resistance is smaller when using liquid Ga as a coolant, with a maximum decrease of 29.8%. Fico's study[12] based on large eddy simulation confirmed that anisotropic effects of the magnetic field are predominant for a turbulent structure in a concentric annular pipe at Ha=60 and Ha=120. Laube[13] experimentally studied the convective heat transfer performance in turbulent liquid metal tube flow with Peclet numbers ranging from 1400 to 3600. The results showed that under non-uniform heat flux conditions, the temperature gradient of the tube wall increased with the increase of Reynolds number, and GaInSn was more pronounced than water. Muhammad[14] numerically analyzed the heat transfer performance of Galinstan in laminar and forced convective flows through a mini-channel heat sink under constant heat flux. It was found that the heat transfer performance of Galinstan in deep and narrow channels is better than that in shallow and wide channels and the heat dissipation rate in the optimized geometry and a flow velocity of 0.21 m/s with a temperature difference of 43 ℃ reaches 158.3 W/cm^2. Wang [15] investigated the convective heat transfer between liquid metal and heated surfaces of micro-channels under an external magnetic field and improved the heat transfer rate by 32%. Zhou [16] investigated the heat transfer performance of nano-liquid-metal (Ga/Cu) in a

circular tube and showed that the heat transfer efficiency of Ga/Cu nano-fluid is 23.8 times that of H_2O/Cu nano-fluid.

Although significant results have been achieved using the above-mentioned methods, the motorized spindle cooling and liquid metal heat dissipation technology are two separate research fields. Meanwhile, few investigations have been carried out on cooling the motorized spindle shaft using liquid metal and circulating liquid metal based on the induced current. Aiming at resolving this shortcoming, an experimental platform is presented and the heat transfer performance of Galinstan liquid metal driven by an electromagnetic field is investigated. Then the cooling effect of liquid metal on the motorized spindle is simulated.

2 Experimental platform and data processing method

2.1 Experimental platform and test conditions

Fig. 2 reveals that the experimental platform mainly consists of a heating subsystem, a cooling subsystem, an electromagnetic drive subsystem, and an acquisition subsystem.

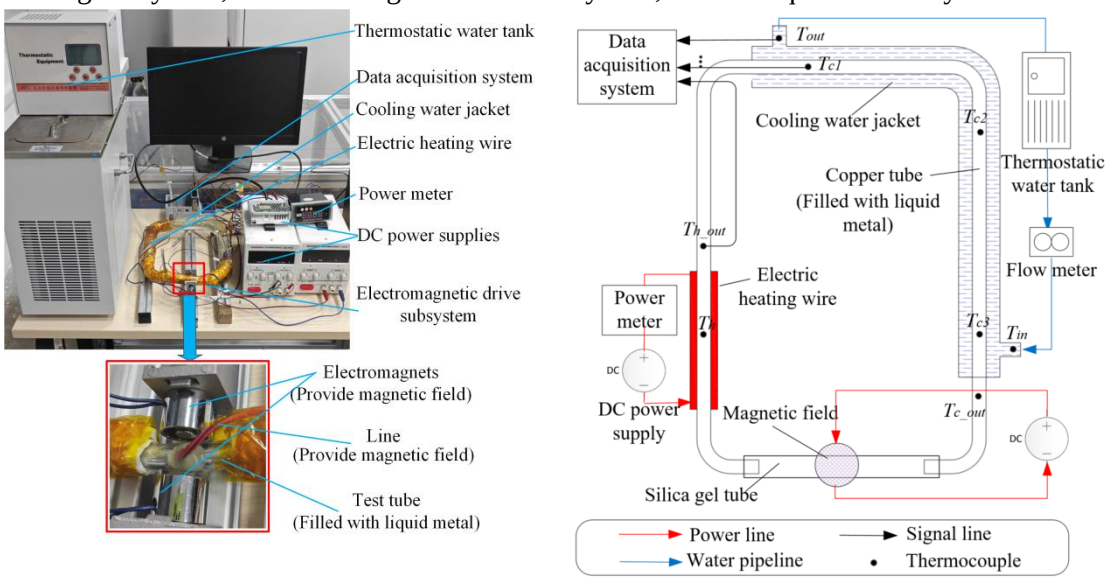

(a) the experimental photographic (b) the experimental layout diagram

Fig. 2 The experimental platform

The heating subsystem is composed of an adjustable DC power supply (*MAISHENG-605D*，*60V, 5A*), a power meter *(FOCUSAI, 200V, 10A)*, and an electric heating wire (*NiCr alloy, 0.2mm*), which is wound on the experimental sample and heats it. The heating power can be adjusted according to the applied voltage to the end of the heating wire. Moreover, the cooling subsystem includes a thermostatic water tank(*QIWEI-DHC-05-B, 30L, ±1℃*), a flowmeter, and a cooling water jacket that wraps around a 350 mm pipe to cool the test sample. The electromagnetic drive subsystem consists of a pair of electromagnets (*SARY, LY-2015, 24V*), an adjustable DC power supply (*MAISHENG-3020D, 30V, 20A*), and some wires. The current provided by the DC power supply replaces the induced current generated by the stator magnetic field of the wire cutting motor. The acquisition subsystem consists of an acquisition board (*NATIONAL INSTRUMENTS, NI-9178, NI-9213*), a computer, and thermocouples(*OMEGA-J, 0-350 ℃*) to record the temperature of the sample during the test.

Six thermocouples are employed to measure the surface temperature of the test sample, and two other thermocouples are employed to measure the inlet and outlet temperature of cooling water. The test specimen is formed by bending a red copper sample with inner and outer diameters of 8mm and 10mm, respectively. The interior of the experimental sample is filled with Galinstan liquid metal. Table 1 shows the physical properties of Galinstan liquid metal at standard conditions.

Table 1. Physical properties of Galinstan liquid metal[17]

Specification	Parameter
Element composition	Ga:In:Sn = 68.5%:21.5%:10%
Density [kg·m]	6363
Viscosity [Pa·s]	0.0022
Thermal conductivity [W/(m·℃)]	23.67+0.061T
Heat capacity [J/(km·℃)]	366 – 0.70T

Considering the performance of the DC power supply in the test platform, its current provided is one of the most important parameters in the test. Accordingly, a simple experimental platform is built as shown in Fig. 3(a). The wire is fixed on the rotating shaft of the motorized spindle and both ends of the wire are connected to the voltage acquisition module. The rated speed and rated current of the motorized spindle (*GDZ*65-1500) are 48000 rpm and 7A, respectively. It is worth noting that there is a speed difference between the motor rotor and stator, which originates from the slip rate of asynchronous motors. The wire installed on the rotating shaft continuously cut the magnetic field of the stator and induces a current. The slip rate of an asynchronous motor used in this mororized spindle is in the range of 2-6%. In the present study, this parameter is set to 5%. Therefore, the rotating speed of the wire at the rated speed is 2400 rpm. Moreover, the current and voltage frequency of the inverter, which are applied to the motor stator, are set to 7A and 40 Hz, respectively.

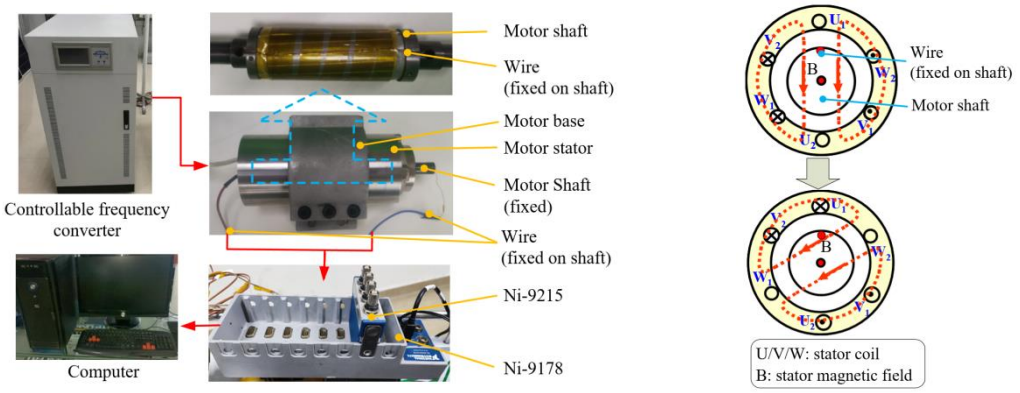

(a) The experimental platform

(b)Schematic diagram of generating induced voltage

Fig. 3 The experimental system for measuring the induced voltage

U, V, and W in Fig.3(b) represent the stator coil windings of the motor. When the frequency converter changes the power supply of the three-phase coil, a rotating magnetic field will be formed inside the motor stator. Under the action of this rotating magnetic field, an induced voltage is formed inside the wire. A acquisition system is employed to measure the induced voltage and the current flowing through the liquid metal can be obtained. The test

results show that with a speed difference of 2400 rpm and a stator current of 7A, the effectively induced voltage in the wire is 1.2V. Therefore, a DC voltage of 1.2V is applied to the circuit shown in Fig. 1(b), which leads to a current of 19.7A passing through the liquid metal. To simplify the calculations, the maximum current used to drive the flow of liquid metal is set to 20A, with 4A as an interval. In this way, when the electric spindle rotates at 9600rpm, 19200rpm, 28800rpm, 39400rpm and 48000rpm, the induced currents flowing through the liquid metal are 4A, 8A, 12A, 16A, 20A, respectively. The experimental conditions and parameters of the test sample are listed in Table 2.

Table 2. Experimental conditions and parameters of the test sample

Specification	Parameter
Working fluid	Galinstan liquid metal
Overall length / width [mm]	275 / 185
Length of heating part [mm]	120
Length of cooling part [mm]	350
Internal / external diameter [mm]	8 / 10
Heating power [W]	40, 80, 120 ...
Mass flow rate of cooling water [g/s]	300±20
Inlet temperature of cooling water [°C]	23±1
Electric current [A]	4, 8, 12, 16, 20
Mounting angle [°]	0

2.2 Data processing and uncertainty analysis

The equivalent heat transfer coefficient (λe) is employed to evaluate the heat transfer performance of liquid metal. This coefficient is defined as follows[9]:

$$\lambda e = \frac{4QL}{\left(\overline{T}_{h\_out} - \overline{T}_{c\_out}\right)\pi d^2} \tag{1}$$

where L=440 mm is the distance between the heating and the cooling sections, d=8 mm is the inner diameter of the test sample, $\overline{T}_{h\_out}$ and $\overline{T}_{c\_out}$ are the average temperatures at the outlet of the heating and cooling sections, respectively. Moreover, Q denotes the heat transferred by the liquid metal.

The heat Q transferred by the cooling water can be calculated using the following expression[9]:

$$Q = \dot{m}C\left(T_{\text{out}} - T_{\text{in}}\right)/60 \tag{2}$$

where $\dot{m}$ is the mass flow rate of the cooling water, C=4.2 J·g^{-1}·°C^{-1} is the specific heat capacity of the cooling water, T_{in} and T_{out} are the inlet and outlet water temperatures, respectively.

In the experiment, the measuring accuracy of L and d was ±0.1 mm, and the measuring precision of the wattmeter was ±0.5%. Meanwhile, the measurement accuracy of the temperature was ±1°C, Q was calculated when P≥120W, and the ratio of Q and P was linearly

fitted using the least square method, resulting in Q=0.88P, wherein the residual error is less than 3.4%.

According to the equipment accuracy and experimental results, uncertainties of the experiment are between 4.6%（I=20A, P=360W）and 9.7% (I=4A, P=40W).

3 Experimental result

3.1 Temperature distribution

Fig. 4 shows the distribution of temperature in the copper test sample under different driving currents. The black curve in the legend represents the heating power, and its step up represents a gradual increase in heating power. It is observed that when I=0, the heating section temperature increases first and then stabilizes slowly. The stable temperature at P = 10W is 94 ℃. Furthermore, the cooling section temperature is not affected by the heating power and is almost constant. Fig. 4(b) shows that when the driving current increases to 4A, the temperature of the heating section rises slightly and then approaches 31 ℃ at P = 40W. Temperature variations of the cooling and heating sections against the heating power are similar and have a step shape.

The heating section temperature is influenced by liquid metal and electric heating wire, and the cooling section temperature is affected by liquid metal and cooling water. When I=0A, due to the absence of electromagnetic force as the power source, the liquid metal does not flow inside the copper tube. In this case, the liquid metal in the heating section heats up and the heating section temperature rises to 94 ℃. Similarly, the cooling section temperature is mainly affected by the constant temperature cooling water, and is almost constant. When I＞0A, both the sharp decrease of the heating section temperature and the step-by-step increase of the cooling section temperature confirm that the electromagnetic force provided by the 4A current drives the flow of liquid metal between the heating and cooling parts of the tube.

When the driving current increases from 4A to 20A, the outlet temperature of heating section (T_{h_out}) decreases from 113 ℃ (I = 4A, P = 400W) to 76 ℃ (I = 20A, P = 400W), while the outlet temperature of cooling section increases from 31 ℃ (I = 4A, P = 400W) to 40 ℃ (I = 4A, P = 400W). According to Ampere's law, the driving force of liquid metal is directly proportional to the magnetic field and the current. During the experiment, the magnetic field remains constant. As the driving current increases from 4A to 20A, the power driving the flow of liquid metal in the tube increases, and the flow speed of liquid metal in the tube also increases. Therefore, when the heating power is the same, the temperature of the heating section is lower at high driving current than at low driving current, while the temperature of the cooling section is exactly the opposite.

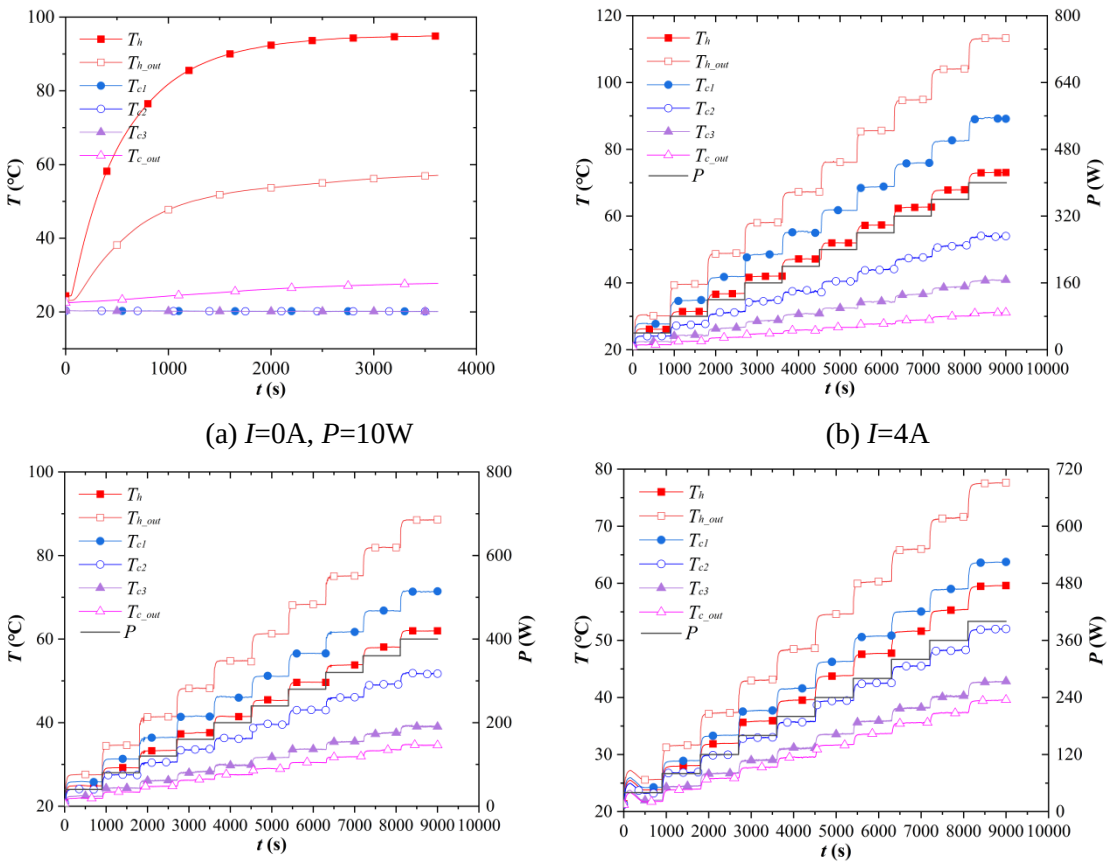

(a) I=0A, P=10W (b) I=4A

(c) I=12A (d) I=20A

Fig. 4 Temperature distribution under different driving currents

3.2 Heat transfer characteristics

The distribution of equivalent thermal conductivity of liquid metal in the copper tube under different driving currents is shown in Fig. 5. It is observed that as the heating power increases, the corresponding equivalent thermal conductivity of the liquid metal under the same driving current remains constant. However, when the driving current increases, the equivalent thermal conductivity of the liquid metal in the copper tube increases significantly. More specifically, when the driving current increases from 4A to 20A, the equivalent thermal conductivity of the liquid metal increases from $3.7*10^4$ W/(m·℃) to $8.1*10^4$ W/(m·℃), which shows an increase of 118%.

It should be indicated that Ampere's force is the power of electromagnetic drive, which is directly proportional to the strength of the magnetic field and current, and the wire length. In other words, Ampere's force is independent of the heating power so the flow rate and heat transfer performance are not affected by the heating power. Fig. 5 shows that as the heating power increases continuously, the equivalent thermal conductivity remains constant. However, when the driving current increases, Ampere's force increase significantly, the electromagnetic driving effect improves, the flow of the liquid metal in the copper tube accelerates, and heat transfer performance improves. Therefore, as the driving current increases from 4a to 20A, the equivalent thermal conductivity between the heating section and the cooling section increases by 118%.

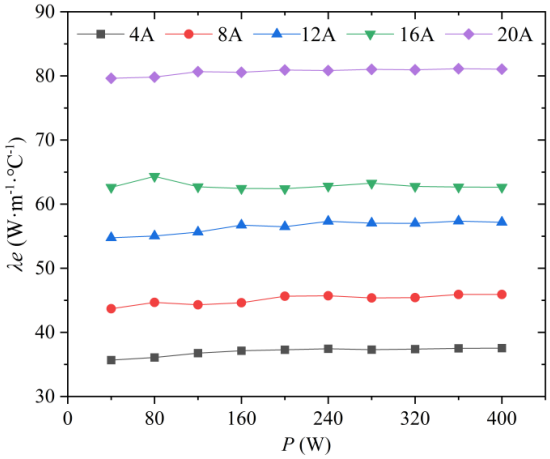

Fig. 5 The equivalent heat conductivity under different driving currents

3.3 Evaluation of the cooling effect of the motorized spindle

Based on the obtained results in the previous section, the equivalent thermal conductivity of the liquid metal in the cooling structure is considered constant. Based on the simulation model of the 150SD motorized spindle [18], the velocity is set to 5000 rpm and properties of the liquid metal are considered for coolant.

Table 3. The values of the boundary conditions

Boundary conditions	**components**	**values**
Motor heat generation [W]	Rotor	267
	Stator	134
Front bearing heat flux [KW/m^2)]	Inner ring raceway	7500
	Rollers	12
	Outer ring raceway	5.4
Rear bearing heat flux [KW/m^2)]	inner ring raceway	6.4
	Outer ring raceway	10
	Rollers	4.3
Convective heat transfer coefficients **[W/(m^2·℃)]**	Stator/Cooling jacket	2046
	Stator/Rotor	96
	Shaft/Air	85
	Spindle outer housing/Air	9.7
Thermal conductivity **[W/(m·℃)]**	38CMoAL	65.5
	Liquid metal	37000
	20Cr (shaft)	44
	GCr15SiMn	60.5

Figs. 6(a)-6(c) show the model of a 150SD motorized spindle with and without an N-pentane loop thermosyphon shaft cooling structure [18]. Moreover, Fig. 6(d) shows the temperature distribution with the liquid metal shaft cooling structure. It is observed that the temperature distribution of the 150SD motorized spindle with a shaft cooling structure is more uniform than that without a shaft cooling structure, and the state of "external cooling

and internal heat" of the motorized spindle is effectively alleviated. The motor and bearings are enclosed inside the motorized spindle by a casing and end cover, resulting in extremely poor heat dissipation. Therefore, the heat generated by the motor and bearings during the operation of the motorized spindle continues to accumulate, causing temperature to continue to rise. Finally, the electric spindle forms a temperature distribution of external cooling and internal heating, with a large temperature gradient. The shaft cooling structure directly cools the motorized spindle rotor system and reduce its temperature, making the temperature of 150SD motorized spindle more uniform. It is found that the liquid metal shaft cooling structure reduces the maximum internal temperature (rotor) from 78.4℃ to 45.7 ℃. which is much more than that of the N-pentane loop thermosiphon.

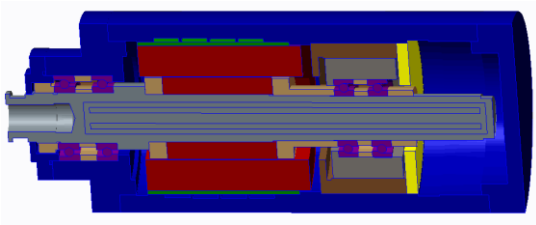

(a) 150SD motorized spindle model

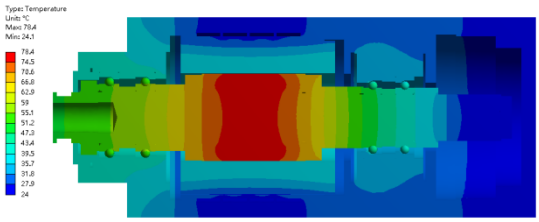

(b) temperature contour without shaft cooling structure

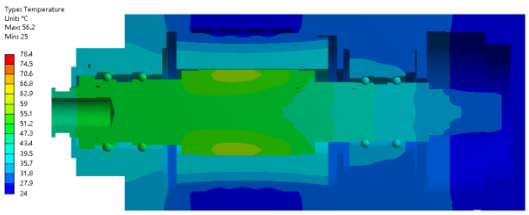

(c) temperature contour with N-pentane loop thermosyphon shaft cooling structure

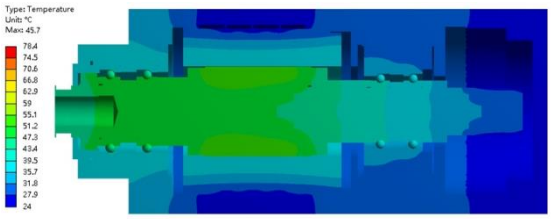

(d) temperature contour with liquid metal shaft cooling structure

Fig. 6. Model and temperature contour of 150SD motorized spindle with different shaft cooling structures

3 Conclusion

In the present study, a motorized spindle shaft cooling structure was designed based on the Galinstan liquid metal as coolant. Then the heat transfer performance of the designed cooling structure was studied experimentally. Based on the performed analyses, the main achievements can be summarized as follows:

(1) The effective induced voltage generated in the wire fixed on the rotating shaft of an asynchronous motor is 1.2V, which induces a current of 20A in the liquid metal. This induced current can circulate the liquid metal in a copper circuit.

(2) It is concluded that the designed structure has extremely high heat transfer performance. And the equivalent thermal conductivity of the liquid metal increases with the increase of driving current. More specifically, as the driving current increases from 4A to 20A,

the equivalent thermal conductivity increases from $3.7*10^4$ W/(m·℃) to $8.1*10^4$ W/(m·℃), which shows an increase of 118%.

(3) The electromagnetic-driven liquid metal shaft cooling structure has a promising cooling effect on the motorized spindle, which can make the temperature distribution of a motorized spindle more uniform. Based on the simulation results, applying the designed structure can reduce the maximum temperature rise of the 150SD motorized spindle at 5000 rpm by 60%.

Acknowledgments

This work was supported by the Guangdong Basic and Applied Basic Research Foundation (No. 2020A1515111099, No.2019A1515110304), the Natural Science Foundation of China(No. 52305459).

Nomenclature

Nomenclature		*Subscripts and superscripts*	
C	*equivalent thermal conductivity* [J/(g ·℃)]	*c*	*cooling section*
d	*diameter* [m]	*h*	*heating section*
L	*distance* [m]	*in*	*inlet*
$\dot{m}$	*mass flow rate* [g/s]	*out*	*outlet*
P	*Heating power* [W]	-	*average*
Q	*heat transfer rate* [W]		
I	*electric current* [A]		
t	*time* [s]		
T	*temperature* [℃]		
λ_e	*equivalent thermal conductivity* [W/(m·℃)]		

Reference

[1] Kim, D.H. , Song J.Y. Development of thermal deformation compensation device and CNC based real-time compensation for advanced manufacturing, *Int J Auto Tech-Kor. 14 (2013), 3*, pp. 423-428.

[2] Zhao, J., Wang, L., Mao, X., et al. Preparation and properties of porous alumina ceramics for ultra-precision aerostatic bearings[J]. *Ceram Int.* 2022(9):48.

[3] Zhao, J., Sheng, W., Li, Z., et al. Effect of lubricant selection on the wear characteristics of spur gear under oil-air mixed lubrication[J]. *Tribol Int, 167(2022),*pp: 107382-1-12.

[4] Belfort, G., Raparelli, T., Trivella, A. CFD analysis of a simple orifice-type feeding system for aerostatic bearing, *Tribol Lett. 58 (2015), 2*. pp. 25-32.

[5] Gohara, M., Somaya, K., Miyatake, M. Static characteristics of a water-lubricated hydrostatic thrust bearing using a membrane restrictor, *Tribol Int. 75 (2014),* pp. 111-116.

[6] Li, A.L., He, Q., Zhang, P.W. Experimental study on cooling system of high-speed grinding spindle, *Machine Tool & Hydraulics. 44 (2016), 9,* pp. 62-65.

[7] Holkup, T., Cao, H., Kolar, P. *et al.* Thermo-mechanical model of spindles. *CIRP Ann-Manuf Techn. 59 (2010), 1,* pp. 365-368.

[8] Kang, Y.R., Shi, X.J., Gao, J.M. *et al*. Thermal behavior analysis of a motorized spindle with novel shaft core cooling, *J. Xi' An Jiaotong Univ. 51(1)(2017)*:13-18.

[9] Li, F.J., Gao, J.M., Shi, X.J. Experimental investigation of an R600a two-phase loop thermosiphon to cool a motorized spindle shaft, *Int Commun Heat Mass. 97 (2018),* pp. 9-16.

[10] Zhang, Y., Wang, L., Zhang, Y., et al. Design and thermal characteristic analysis of motorized spindle cooling system:[J]. *Adv Mech Eng, 13(2021),* pp:781-802.

[11] Xiang X , Liu W , Fan A .Comparison between the cooling performances of micro-jet impingement systems using liquid metal and water as coolants for high power electronics[J].*Int J Therm Sci, 173(2022),*pp:107375.

[12] Fico, F., Langella, I. Large-eddy simulation of magnetohydrodynamics and heat transfer in annular pipe liquid metal flow[J]. *Phys Fluids, 35(2023),*pp:55106.

[13] Laube, T., Dietrich, B., Marocco, L., et al. Turbulent heat transfer in a liquid metal tube flow with azimuthally inhomogeneous heat flux[J]. *Int J Heat Mass Trans, 189(2022),* pp:122734.

[14] Muhammad, A., Selvakumar, D., Wu, J. Numerical investigation of laminar flow and heat transfer in a liquid metal cooled mini-channel heat sink. *Int J Heat Mass Trans. 150 (2020),* pp. 119265.1-119265.9.

[15] Wang, Z.H., Lei, T.Y. Liquid metal MHD effect and heat transfer research in a rectangular duct with micro-channels under a magnetic field. *Int J Therm Sci. 155 (2020),* pp. 106411.

[16] Zhou, X.M., Li, X.F., Cheng K.Y. Numerical study of heat transfer enhancement of nano liquid-metal fluid forced convection in circular tube. *J Heat Trans-T ASME. 140 (2018), 8,* pp. 145-157.

[17] Muhammad, A., Selvakumar, D., Wu, J. Numerical investigation of laminar flow and heat transfer in a liquid metal cooled mini-channel heat sink[J]. *Int J Heat Mass Trans. 150(2020)*:119265.1-119265.9.

[18] Zhang, X.D., Yang, X.H., Zhou, Y.X., et al. Experimental investigation of galinstan based minichannel cooling for high heat flux and large heat power thermal management[J]. *Energ Convers Manage, 185(2019),*pp:248-258.

Paper submitted: 16.09.2023
Paper revised: 23.10.2023
Paper accepted: 01.11.2023